Available online at www.sciencedirect.com

ScienceDirect

IFAC Papers Online CONFERENCE PAPER ARCHIVE

IFAC PapersOnLine 50-1 (2017) 15773–15779

Observability measurement and control strategy for induction machine sensorless drive in traction applications

G. Lefebvre [*,**] **X. Lin-Shi** [**] **M. Nadri** [***] **J.-Y. Gauthier** [**] **A. Hijazi** [**]

[*] *Alstom, Villeurbanne, France (e-mail: gaetan.lefebvre@alstom.com)*
[**] *Université de Lyon - Laboratoire Ampère - INSA Lyon, Villeurbanne, France (e-mail: xuefang.shi@insa-lyon.fr, jean-yves.gauthier@insa-lyon.fr, alaa.hijazi@insa-lyon.fr)*
[***] *Université de Lyon - LAGEP, Villeurbanne, France (e-mail: nadri@lagep.univ-lyon1.fr)*

Abstract: Electrical traction using induction machine sensorless control requires high observer performance for all speed ranges, even for low speed or regenerative braking conditions which appear frequently during long time. It is well known that the speed of induction motors is unobservable at very low stator frequencies. This paper uses an observability index to continuously analyze speed observability for sensorless control of induction machines. The correlation between observability-index and observer performance is illustrated in a Hardware in the Loop (HIL) experimental test-bench combining the well-known vector control with an extended Kalman filter. Thanks to the observability-index information, an optimal strategy is proposed to design controllers to guide the system away from undesirable behavior and avoid the weak observability-index region by taking into account all working constraints. A simplified case is presented to improve the speed observer performance, which was tested in the same conditions with the same HIL test-bench to experimentally validate the proposed sensorless control for traction applications.

Keywords: Railway electric traction, induction machine sensorless drive, observability analysis, electric automotive control, application of power electronics.

1. INTRODUCTION

To reduce the number of physical sensors, and the direct and maintenance costs they induce, industrial solutions have been based on state observers for years. For an induction machine drive, the speed sensor is the most critical because of its cost and its high failure rate compared to current and voltage sensors. In the case of a traction application, the high failure rate of the speed sensor is mainly caused by the harsh environment (vibration, impacts, temperature...). However, in this application, it is compulsory to have a precise sensorless drive on the entire speed and torque range. The problem of the speed sensorless induction machine drive has been first addressed in the 1980s (Tamai et al. (1985)). Such a drive nevertheless suffers from one major drawback for an industrial application: it cannot in the same time be adapted to any kind of induction machine and regulate the torque precisely on the whole speed range (Kim and Sul (2011)). This is due, on one hand, to speed unobservability when the fundamental modeling is used with the aim of an application to a wide kind of induction machines, and on the other hand, to the dependency to the machine geometry of high frequency injection methods used to get additional speed information at very low stator frequency. The critical points are known to be around zero stator frequency (Canudas De Wit et al. (2000)), and the difficulty will be all the higher as it remains in this area for a long time. For a railway traction application, this corresponds to an electrical braking up to zero speed or to a rollback start, when the speed takes negative values while the torque takes positive ones, the equivalent of a hill start in an automotive application. While (Ghanes et al. (2006)) proposes a way to ensure the stability of speed observation during these phases that can be adapted easily to any kind of induction machine, it does not permit to ensure the precision and the dynamic of this observation for a long rollback start. In a railway application, rollback starts can take as long as tenths of seconds.

In this paper, a deep analysis of the observability is undertaken and used to design a control approach taking into account continuous observability measurements. The weak observability avoidance strategy proposed in this work can be easily implemented for different industrial uses of induction machines speed sensorless drive such as in traction application.

The paper is organized as follows: after some preliminaries, an observability analysis and its continuous measurement for nonlinear systems are presented in section 2, the application to the case of an induction machine is studied in section 3. Section 4 uses this continuous observability

2405-8963
Peer review under responsibility of International Federation of Automatic Control.
10.1016/j.ifacol.2017.08.2312

measurement to analyze more precisely the speed observability evolution. Section 5 proposes a general approach to take into account observability in a control. A weak observability-index avoidance strategy tested in railway traction case shows that it is possible to use a speed sensorless drive to control the torque precisely on the whole speed range, including during a rollback start.

2. PRELIMINARIES

The study of system observability and controllability can be traced back to the development of state space representations by Kalman (Kalman (1960)). Although these concepts have been widely used for the study of linear systems, their applicability to the analysis of nonlinear systems was limited. In the 1970s, major works by Hermann and Krener (Hermann and Krener (1977)) and Sussmann (Sussmann (1976)), presented alternative means to study the observability of nonlinear systems. These approaches relied on Lie algebra and geometric control theory.

2.1 Observability analysis : Lie derivative

In a nonlinear system, the traditional approach of identifying the observability through the use of an observability gramian fails. However, the observability of nonlinear systems may be evaluated by the analysis of the rank condition of the observability matrix using Lie derivatives (Hermann and Krener (1977)).

Considering the nonlinear system Σ

$$\Sigma : \begin{cases} \dot{x} = f(x,u) \\ y = h(x), \end{cases} \tag{1}$$

where the state x is in $\mathbb{R}^n$; $u \in \mathbb{R}^m$ is the control signal; $y \in \mathbb{R}^p$ is the output vector and f and h are nonlinear function of suitable dimensions. The observability matrix of the system $\mathcal{O}_\Sigma$ is given by

$$\mathcal{O}_\Sigma = \frac{\partial L}{\partial x}, \tag{2}$$

where L is the observation space of the system :

$$L = \begin{bmatrix} \mathcal{L}_f^0 h \\ \mathcal{L}_f^1 h \\ \vdots \\ \mathcal{L}_f^p h \end{bmatrix} \text{ and } \begin{cases} \mathcal{L}_f^0 h = h \\ \mathcal{L}_f h = \frac{\partial h}{\partial x} f \\ \forall k \in \mathbb{N}^*, \mathcal{L}_f^k = \mathcal{L}_f(\mathcal{L}_f^{k-1} h) \end{cases} \tag{3}$$

Theorem 1. (Hermann and Krener (1977)) : If system (1) satisfies the observability rank condition at x_0, it is locally weakly observable at x_0.

The observability rank condition is necessary and sufficient as soon as the system is weakly controllable (Hermann and Krener (1977), Theorem 3.12), which covers most cases. In almost all cases, it is thus correct to identify as unobservable points those for which the rank condition is not respected. Indeed, the notion of a measurement of observability has additional significance for nonlinear systems, where certain sections of the system trajectory may correspond to unobservable regions for a given output equation. One of the methods for evaluating the observability (continuously) of a nonlinear system is based on the use of Lie derivatives evaluated at various locations along the system trajectory.

The first element to notice is that this concept can only provide qualitative results (binary information) on the observation system. Obviously, quantitative measurement of observability i.e. an information of how far a system is from becoming unobservable, is a key issue in practical applications on state estimation theory.

2.2 Observability measurement : observability index

The problem of a continuous measurement of observability has been treated for linear systems using both the observability matrix and the observability gramian (Müller and Weber (1972)). Among the proposed measurements, such as the observability of the least observable state (minimum eigenvalue of the observability matrix or gramian), or a mean observability of the system (determinant and trace of the observability matrix or gramian), each one can give a different part of the information. No one can be seen as the best observability continuous measurement. Its interest is nevertheless limited in real application since, for a linear system, the observer tuning is done only once and does not depend on the working point of the system.

For nonlinear systems, the information of a continuous measurement of observability offers more perspective for observer or control tuning. However a similar definition is more complicated to get and to prove. The definitions found in the literature mainly use the observability matrix (Böhm et al. (2008)) or the empirical observability gramian (Krener and Ide (2009), Singh and Hahn (2006)). The empirical observability gramian, described in (Lall et al. (2002)), provides a numeric value of the observability. Its result is relevant for a given point or trajectory. On the other hand, the observability matrix provides an analytic value that remains relevant for all points or trajectories. Thus, we chose to use the observability matrix to define the observability continuous measurement.

Once the matrix used to support the definition has been chosen, the quantitative measurement of observability remains to be defined. The same way than for linear systems, three criteria can be used : the minimum eigenvalue, the trace or the determinant. The similar need to reduce the information contained in a matrix to a scalar number exists for identification problems using the sensibility matrix (Qian et al. (2014)). We can thus refer to these works to select the most interesting criteria (Franceschini and Macchietto (2008)). The use of the determinant of the matrix is presented as the most significant since it considers the confidence in the observation of the global system, considering the errors committed on each state weighted by the sensibility of the observation to this given state. This criterion is also invariant with re-scaling transformations and it is the most used.

Definition 1. (Observability index) the continuous measurement of the observability of the system Σ, η_Σ, is :

$$\eta_\Sigma = \det(\mathcal{O}_\Sigma^T \mathcal{O}_\Sigma), \tag{4}$$

where $\mathcal{O}_\Sigma$ is the observability matrix given by (2).

The larger this value is, the farther the system will be from unobservable region.

Remark 1. The important point is that the determinant of the observability matrix (2) tends to zero when approaching unobservable regions i.e. the correction term

measuring the deviation between the observed value and its observer prediction diverges from the physical domain. This may compromise the recovery of the state vector using an "closed-loop" observer. Indeed, in this conditions, a switch to the estimator version has been used in some practical applications (Ghanes et al. (2006)) when system is still detectable and the external perturbations are small.

However, the measurement and model noises will be amplified which makes the observer diverge. This remains whatever the observer type or tuning. Selecting a particular observer or working on the observer tuning is thus a vain work when dealing with an unobservable working point.

Based on Remark 1, the divergence of the observer may thus appear in the neighborhood of an unobservable working point. A continuous measurement of the observability may be an important information to know the width of this problematic neighborhood.

3. OBSERVABILITY CONTINUOUS MEASUREMENT FOR INDUCTION MACHINE

3.1 Induction machine models

Induction machine used for railway electric traction is a classical one where the electrical part is frequently modeled using the stator currents and rotor flux. Generally the electrical speed ω can be assumed nearly constant with respect to the currents and flux dynamics. Thus, in the stationary reference frame (α, β), induction machine can be modeled as (5)

$$\Sigma_{IM_{(\alpha,\beta)}}: \begin{cases} \dot{i}_{s\alpha} = -\left(\frac{R_s}{L_\sigma} + \frac{L_m^2 R_r}{L_\sigma L_r^2}\right) i_{s\alpha} + \frac{L_m R_r}{L_\sigma L_r^2}\varphi_{r\alpha} \\ \qquad + \frac{L_m \omega}{L_\sigma L_r}\varphi_{r\beta} + \frac{v_{s\alpha}}{L_\sigma} \\ \dot{i}_{s\beta} = -\left(\frac{R_s}{L_\sigma} + \frac{L_m^2 R_r}{L_\sigma L_r^2}\right) i_{s\beta} - \frac{L_m \omega}{L_\sigma L_r}\varphi_{r\alpha} \\ \qquad + \frac{L_m R_r}{L_\sigma L_r^2}\varphi_{r\beta} + \frac{v_{s\beta}}{L_\sigma} \\ \dot{\varphi}_{r\alpha} = \frac{L_m R_r}{L_r} i_{s\alpha} - \frac{R_r}{L_r}\varphi_{r\alpha} - \omega\varphi_{r\beta} \\ \dot{\varphi}_{r\beta} = \frac{L_m R_r}{L_r} i_{s\beta} + \omega\varphi_{r\alpha} - \frac{R_r}{L_r}\varphi_{r\beta} \\ \dot{\omega} = 0 \end{cases} \quad y = [i_{s\alpha}, i_{s\beta}]^T \tag{5}$$

where $(i_{s\alpha}, i_{s\beta})$ are the stator currents in the (α,β) reference frame, $(\varphi_{r\alpha}, \varphi_{r\beta})$ are the rotor flux, $(u_{s\alpha}, u_{s\beta})$ are the stator voltages. R_r and R_s are respectively the rotor and stator resistances, L_r, L_m and L_σ are respectively the rotor, magnetizing and leakage inductances, and ω_s is the frequency of the stator currents.

For control purpose, the rotating reference frame (d, q) is used. The model in this reference frame is given in (6)

$$\Sigma_{IM_{(d,q)}}: \begin{cases} \dot{i}_{sd} = -\left(\frac{R_s}{L_\sigma} + \frac{L_m^2 R_r}{L_\sigma L_r^2}\right) i_{sd} + \omega_s i_{sq} + \\ \qquad \frac{L_m R_r}{L_\sigma L_r^2}\varphi_{rd} + \frac{L_m \omega}{L_\sigma L_r}\varphi_{rq} + \frac{u_{sd}}{L_\sigma} \\ \dot{i}_{sq} = -\omega_s i_{sd} - \left(\frac{R_s}{L_\sigma} + \frac{L_m^2 R_r}{L_\sigma L_r^2}\right) i_{sq} - \\ \qquad \frac{L_m \omega}{L_\sigma L_r}\varphi_{rd} + \frac{L_m R_r}{L_\sigma L_r^2}\varphi_{rq} + \frac{u_{sq}}{L_\sigma} \\ \dot{\varphi}_{rd} = \frac{L_m R_r}{L_r} i_{sd} - \frac{R_r}{L_r}\varphi_{rd} + (\omega_s - \omega)\varphi_{rq} \\ \dot{\varphi}_{rq} = \frac{L_m R_r}{L_r} i_{sq} - (\omega_s - \omega)\varphi_{rd} - \frac{R_r}{L_r}\varphi_{rq} \\ \dot{\omega} = 0 \end{cases} \quad y = [i_{sd}, i_{sq}]^T \tag{6}$$

where (i_{sd}, i_{sq}) and $(\varphi_{rd}, \varphi_{rq})$ are respectively the stator currents and the rotor flux in the (d,q) reference frame.

In a sensorless application, the only measured states are the two currents, indirectly measured from the phase current measurements. The observed variables are the flux and the speed. In the following, the observabilty of the nonlinear systems (5) and (6) will be studied.

3.2 Induction machine observability analysis

Considering that the only measured states are the two currents, the observability matrix can be obtained by these currents and their two first Lie derivatives.

For the model $\Sigma_{IM_{(\alpha,\beta)}}$, a base change has been done to allow a simpler representation following

$$\mathcal{O}_{\Sigma_{IM_{(\alpha,\beta)}}} = \begin{bmatrix} 1 & 0 & 0 & 0 & 0 \\ 0 & 1 & 0 & 0 & 0 \\ 0 & 0 & \frac{R_r}{L_r} & \omega & \varphi_{r\beta} \\ 0 & 0 & -\omega & \frac{R_r}{L_r} & -\varphi_{r\alpha} \\ 0 & 0 & 0 & 0 & \dot{\varphi}_{r\beta} \\ 0 & 0 & 0 & 0 & -\dot{\varphi}_{r\alpha} \end{bmatrix}. \tag{7}$$

The observability rank condition is satisfied if $(\dot{\varphi}_{r\alpha}, \dot{\varphi}_{r\beta}) \neq (0,0)$. Considering the flux vector $\boldsymbol{\varphi}_r$, this condition can be expressed as (8) which corresponds to non constant flux vector.

$$\dot{\varphi}_{r\alpha} \neq 0 \cup \dot{\varphi}_{r\beta} \neq 0 \Rightarrow \dot{\varphi}_{r\alpha} + j\dot{\varphi}_{r\beta} \neq 0 \Rightarrow \dot{\boldsymbol{\varphi}}_r \neq 0 \tag{8}$$

If the module of this vector is constant, i.e. in constant flux operations, it is sufficient that its rotation angle is not-zero to respect the observability condition. In other words, the state vector is observable while the stator frequency ω_s remains non-zero. This is in concordance with the observability conditions presented in the literature (Vaclavek et al. (2013), Ghanes et al. (2006)). As noticed in (Ghanes et al. (2006)), higher derivation terms would involve flux derivations of second order and more that would not modify the observability condition.

For the model $\Sigma_{IM_{(d,q)}}$, another base change leads to a simple form of the observability matrix as (9).

$$\mathcal{O}_{\Sigma_{IM_{(d,q)}}} = \begin{bmatrix} 1 & 0 & 0 & 0 & 0 \\ 0 & 1 & 0 & 0 & 0 \\ 0 & 0 & \frac{R_r}{L_r} & \omega & 0 \\ 0 & 0 & -\omega & \frac{R_r}{L_r} & -\varphi_{rd} \\ 0 & 0 & 0 & 0 & \omega_s\varphi_{rd} \\ 0 & 0 & 0 & 0 & -\dot{\varphi}_{rd} \end{bmatrix} \tag{9}$$

The flux on the d axes, φ_{rd}, corresponds to the amplitude of the flux vector, $\boldsymbol{\varphi}_r$. Thus, in constant flux operations, the state vector is observable while the stator frequency ω_s remains non-zero. This is in concordance with the observability conditions presented in (8) even if the reference frame changed.

3.3 Observability index for induction machine

Using Definition 1 and the observability matrix from (7), the observability index of a sensorless induction machine, $\eta_{\Sigma_{IM_{(\alpha,\beta)}}}$, is presented in (10).

$$\eta_{\Sigma_{IM_{(\alpha,\beta)}}} = \left(\left(\frac{R_r}{L_r}\right)^2 + \omega^2\right)^2 (\varphi_{r\alpha}\dot{\varphi}_{r\beta} - \varphi_{r\beta}\dot{\varphi}_{r\alpha}) \quad (10)$$

Using definition of (4) and the observability matrix from (9), the observability index of a sensorless induction machine, $\eta_{\Sigma_{IM_{(d,q)}}}$, is presented in (11).

$$\eta_{\Sigma_{IM_{(d,q)}}} = \left(\left(\frac{R_r}{L_r}\right)^2 + \omega^2\right)^2 (\omega_s^2\varphi_{rd}^2 + \dot{\varphi}_{rd}^2) \quad (11)$$

Using the flux vector $\boldsymbol{\varphi_r}$ independently of the frame to represent it, the observability index is expressed in (12).

$$\eta_{\Sigma_{IM}} = \left(\left(\frac{R_r}{L_r}\right)^2 + \omega^2\right)^2 (\boldsymbol{\varphi}_r \wedge \dot{\boldsymbol{\varphi}}_r) \quad (12)$$

The flux amplitude $|\boldsymbol{\varphi}_r|$ is generally a constant value, and the speed is set by the used conditions. So, the observability index can be reduced to a value η_1 defined in (13) that represents the same observability information as (11), but is easier to calculate. This value will be used for the rest of the paper.

$$\eta_1 = (\omega_s|\boldsymbol{\varphi}_r|)^2 \quad (13)$$

In the (d,q) reference frame, the (d) axis is oriented with the flux. All the flux is given by φ_{rd} and $\varphi_{rq} = 0$. So, it becomes possible to express the slip frequency ω_r (14). The electrical torque T_e is given in (15), where N_p represents the number of pole pairs.

$$\omega_r = \omega_s - \omega = \frac{R_r L_m}{L_r}\frac{i_{sq}}{|\boldsymbol{\varphi}_r|} \quad (14)$$

$$T_e = \frac{N_p L_m}{L_r}|\boldsymbol{\varphi}_r| i_{sq} \quad (15)$$

The observability index can be expressed, using (14) and (15), as a function varying with the flux amplitude $|\boldsymbol{\varphi}_r|$, the torque, and the speed, as expressed in (16). It gives the possibility to analyze the induction machine observability index depending on these values.

$$\eta_1 = \left(\omega|\boldsymbol{\varphi}_r| + \frac{R_r}{N_p}\frac{T_e}{|\boldsymbol{\varphi}_r|}\right)^2 \quad (16)$$

4. OBSERVABILITY-INDEX ANALYSIS FOR A CLASSICAL SENSORLESS CONTROL

The definition of the observability index enables the analysis of the observability of an induction machine in a sensorless application. The case of a classical field-oriented sensorless control is considered on a hardware in the loop (HIL) experimentation.

The environment of the HIL set-up is presented in Fig. 1. The control is implemented in a real electronic system used on board. All the control is running in real time. The inverter, the induction machine and the voltage, current and speed sensors are simulated in the simulator. For the mechanical part, a 12‰ slope of rail is introduced to simulate the slow down of the speed evolution. From the corresponding inertia, an equivalent load torque is added. It's composed of two 250 kW induction machines in parallel controlled by the same inverter. The induction machine parameters are given in Table 1. This HIL simulator is close enough to a real induction machine to be used by ALSTOM for a large part of the control validation. The control is a kind of field-oriented control (Leonhard (1990)) adapted to the particularities of a railway application. The speed observer is an extended Kalman filter similar to the one presented in (Barut et al. (2007)).

Table 1. Induction machine parameters

Nominal power	P	250 kW
Nominal flux	φ_{nom}	0.808 Wb
Nominal torque	T_{nom}	2160 N.m
Maximum speed	ω_{max}	333 Hz
Pole pair number	N_p	3
Magnetizing inductance	L_m	6.463 mH
Leakage inductance	L_σ	1.174mH

Fig. 1. Environment of the HIL set-up.

The designed observer is based on the model in the (α,β) reference frame given in (5), where the measured states are the two currents, $i_{s\alpha}$ and $i_{s\beta}$, obtained from the phase current measurements.

The observability index η_1 of the induction machine is presented in the (speed, torque) map (Fig. 2) where the flux remains constant at its nominal value. The observability-index variations higher than $300\,\mathrm{Wb^2{\cdot}rad^2{\cdot}s^{-2}}$ have not been represented. The unobservability line presented in (Canudas De Wit et al. (2000)) can be seen considering the zero-observability-index points. It can be remarked that the observability-index map provides information around this unobservability line. It is very interesting to study the observer behavior when the chosen test profile crosses the weak observability zone as the line presented over the observability-index map in Fig. 2.

This test profile corresponds to a rollback start with full-load speed reversal when the train is on a slope rail.

The electrical speed is initialized to about -9 Hz and the torque reference is set to maximal torque. As there are two machines the torque is multiplied by 2 compared to the torque value presented in Fig. 2.

At first, in order to evaluate the speed observation performance, the observed speed is in open-loop with the control which uses an encoder. The results of this HIL

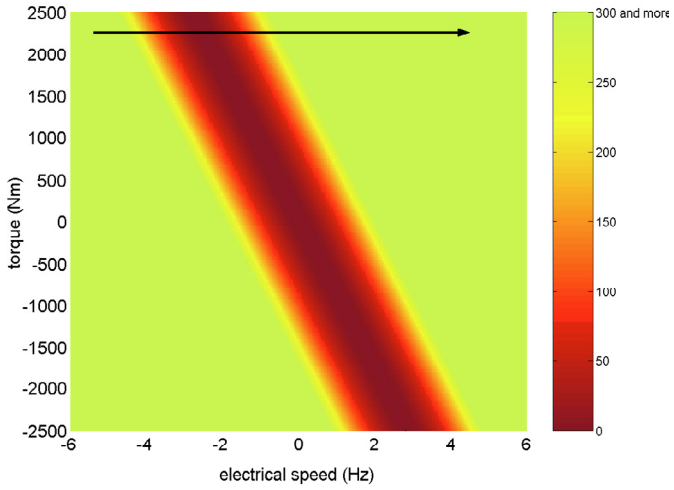

Fig. 2. Observability index η_1 using a classical control.

experiment are presented in Fig. 3. It can be seen a great speed observation error of about 3 Hz and a fall of the observed flux amplitude by more than 50% when the low-observability area is crossed (speed between -4 and 0 Hz).

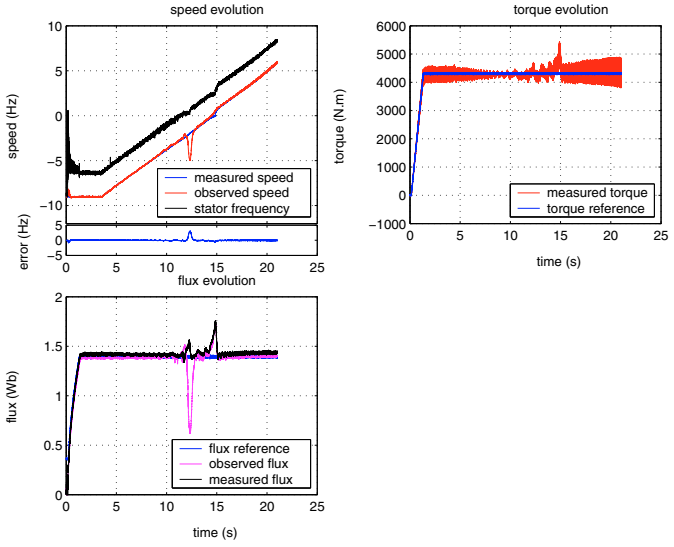

Fig. 3. open-loop result with a classical control.

Then the closed-loop operation is performed. HIL experiments presented in Fig. 4 show that the observed speed is diverged when stator frequency is near to zero. The torque and the flux fall.

These HIL experiments show that when the observability index decreases, the observer performance decreases. The sensorless control is impractical. How to maintain the observability index above a given threshold to guarantee observer performance without degradation of other control constraints? This is the subject of the next section.

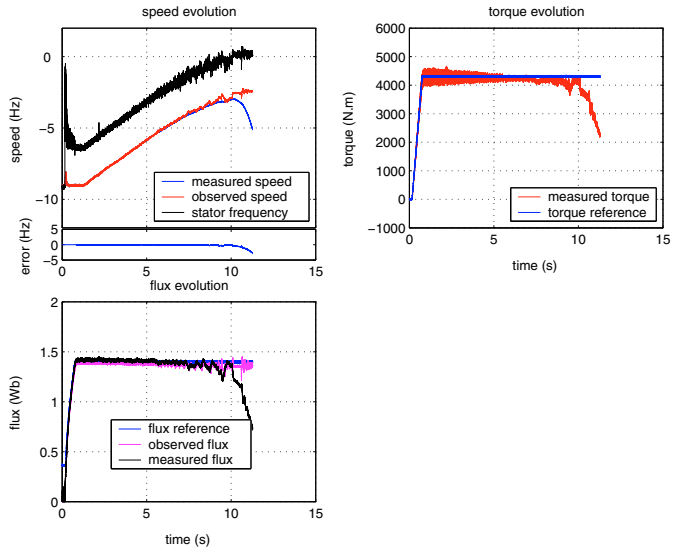

Fig. 4. closed-loop result with a classical control.

5. WEAK OBSERVABILITY-INDEX AVOIDANCE CONTROL

5.1 Avoidance control strategy

When a system Σ reaches an unobservable point, it has been demonstrated that no tuning of the observer may prevent an observer from diverging. The only possible tuning is to annul the observation. In this case, the state vector will be estimated, which will deteriorate the precision of the observation and its resilience to model noises.

The purpose of the weak observability-index avoidance control strategy is to control the system in order to avoid any unobservable point or trajectory. The observer divergence will actually be avoided. It is also possible to avoid not only the unobservable point, but also the points in its neighborhood. To do so, the definition of the observability continuous measurement proposed previously will be a very useful tool.

In most industrial applications, such an avoidance control strategy will force to do a trade-off between the control precision, the observer accuracy and some external constraints, for example the control limit, consumption... This trade-off can be done by minimizing a cost function J that includes at least the state variable error and the observability continuous measurement (Böhm et al. (2008)), (Lefebvre et al. (2015)).

$$J(x(O),u,T)=\int_O^T (x(\tau)-\bar{x}(\tau))^T Q(x(\tau)-\bar{x}(\tau))+\frac{1}{\eta_\Sigma(x(\tau),u(\tau))}\mathrm{d}\tau \tag{17}$$

where $\bar{x}(\tau)$ is the state reference at time τ and Q a weighting matrix. The optimal control on a period T, $u^*(T)$, is given by (18).

$$u^*(T)=\underset{u}{\operatorname{argmin}}(J(x(O),u,T)) \tag{18}$$

In the case of an induction machine sensorless drive, the flux amplitude is a degree of freedom allowing to realize this trade-off. It will be done between the torque precision,

the current consumption and the observability index, as stated in (19), where $|I|$ is the current amplitude, T_e the electrical torque, $T_e^{\#}$ the electrical torque reference, and κ_1 and κ_2 are two coefficients to tune the avoidance control performance.

$$J(|\boldsymbol{\varphi}_r|) = |I|^2 + \kappa_1 (T_e^{\#} - T_e)^2 + \kappa_2 \frac{1}{\eta_1} \tag{19}$$

If no trade-off is expected, an other possibility is to analyze the observability continuous measurement and to adapt *manually* the control. It is well adapted when one criteria has to be strictly respected, whatever the values taken by the others. It can also reduce the computational cost of the avoidance control strategy. In the following, the points corresponding to a low observability-index will be avoided.

5.2 Observability-index based control

As previously underlined, the observability index presented in (16) is a function of the flux amplitude $|\boldsymbol{\varphi}_r|$, the speed ω and the torque T_e. To get an observability-index higher than a given value α, it must ensure the inequality (20) while respecting the other physical constraints of the control.

$$\eta_1 \geq \alpha \Leftrightarrow \left(\omega|\boldsymbol{\varphi}_r| + \frac{R_r}{N_p}\frac{T_e}{|\boldsymbol{\varphi}_r|}\right)^2 \geq \alpha \tag{20}$$

A flux controller is added in the classical vector control to generate the torque and the flux reference as detailed in (Lefebvre et al. (2016)).

To show the effectiveness of the proposed control, its observability index is analyzed in the same way as that described in Section 4.

Fig. 5 presents the evolution of the observability index in the (speed, torque) map when the control of the flux is used for $\alpha = 66{,}7\,\mathrm{Wb}^2{\cdot}\mathrm{rad}^2{\cdot}\mathrm{s}^{-2}$.

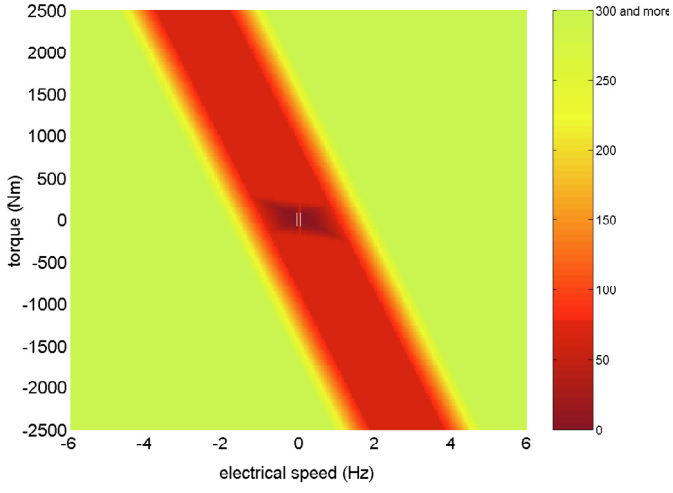

Fig. 5. Observability index η_1 using the proposed control strategy.

Thanks to the proposed control, the weak observability-index zone is considerably reduced compared to that of Fig. 2. It takes as minimal value the value of α fixed to $66{,}7\,\mathrm{Wb}^2{\cdot}\mathrm{rad}^2{\cdot}\mathrm{s}^{-2}$. A small zero observability-index region appears at very low torque and speed conditions because it is not possible to reduce the flux below the minimal threshold φ_{min}. In this case, an injection method can be used to increase the observability index.

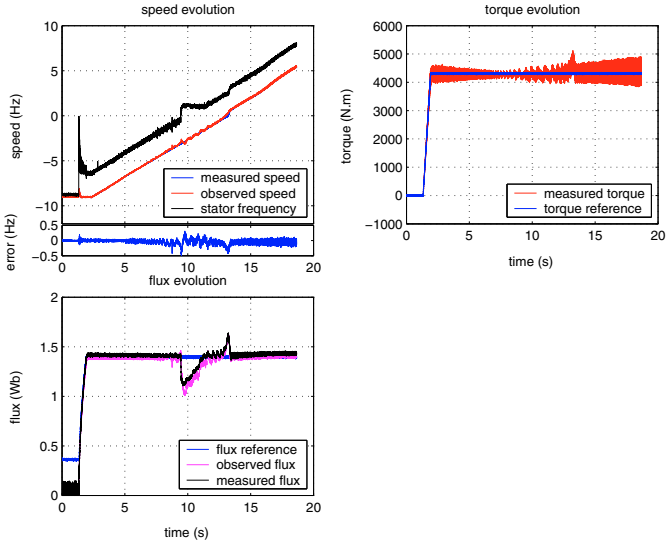

Fig. 6. Open-loop HIL experimental result with the proposed control strategy.

5.3 Open-loop HIL experiment

Using the same observer with the same tunings, the proposed control is implemented for the same profile as Section 4. Fig. 6 presents the results of this HIL experiment. On this figure, it can be seen that the speed observation error remains lower than 0,5 Hz on the whole profile. When the stator frequency crosses zero value, the amplitude of the flux decreases thanks to the proposed control strategy which increases the observability index. The real torque tracks the reference torque, whereas the observed speed keeps following the measured speed. When the observability index becomes important enough again, the flux finds its initial value.

This result shows that by increasing the observability index, it is effectively possible to improve the state observation performance of the induction machine.

5.4 Closed-loop HIL experiment

The observed speed is now used in the closed-loop control. This is an effective induction machine sensorless drive performed on the same test profile whose results are presented in Fig. 7.

As for the open-loop results, the amplitude of the flux decreases to increase the observability index when the stator frequency is near to zero. The speed observation errors are less than 0,5 Hz during all the low speed region. This allows the tracking of the torque reference by the real torque.

These HIL experiments show that the proposed control strategy is an effective solution to perform a sensorless control for induction machine.

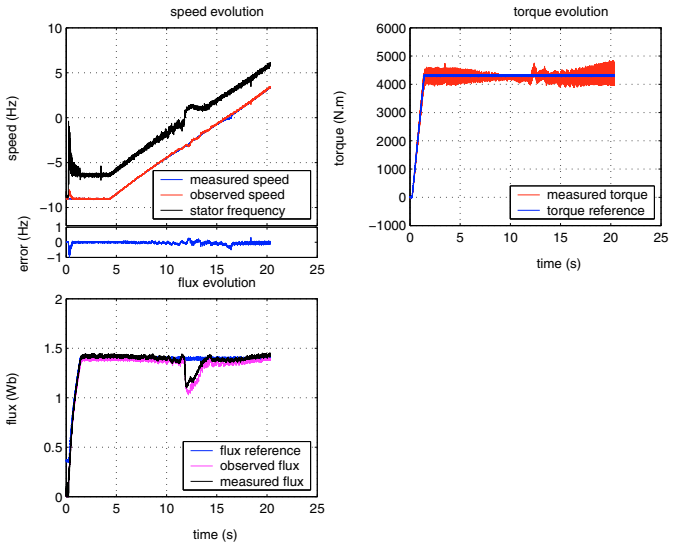

Fig. 7. Closed-loop HIL experiment using the proposed control strategy.

6. CONCLUSION

This paper proposed to go deeper in the observability analysis of induction machine sensorless in order to define an observability continuous measurement. Its application to induction machine sensorless drive evidences two main results: first, the direct link between the observation accuracy and the observability continuous measurement is highlighted; second, this measurement has been considered in the control in order to avoid the weak observability region. The proposed control strategy is illustrated through a simplified case named *observability-index based control* applied to induction machine sensorless drive. Experimental results on a HIL test-bench validate the proposed control for realistic railway traction conditions. It shows that the proposed control can ensure the accuracy and the dynamic of the speed observation, particularly for low speed conditions during long time. The proposed control approach has the potential to be applied easily to any kind of induction machine.

REFERENCES

Barut, M., Bogosyan, S., and Gokasan, M. (2007). Speed-sensorless estimation for induction motors using extended kalman filters. *IEEE Transactions on Industrial Electronics*, 54(1), 272–280. doi:10.1109/TIE.2006.885123.

Böhm, C., Findeisen, R., and Allgöwer, F. (2008). Avoidance of poorly observable trajectories: A predictive control perspective. In *Proceedings of the 17th IFAC World Congress*, 1952–1957. doi:10.3182/20080706-5-KR-1001.00332.

Canudas De Wit, C., Youssef, A., Barbot, J.P., Martin, P., and Malrait, F. (2000). Observability conditions of induction motors at low frequencies. In *Decision and Control, 2000. Proceedings of the 39th IEEE Conference on*, volume 3, 2044–2049 vol.3. doi:10.1109/CDC.2000.914093.

Franceschini, G. and Macchietto, S. (2008). Model-based design of experiments for parameter precision: State of the art. *Chemical Engineering Science*, 63(19), 4846–4872. doi:10.1016/j.ces.2007.11.034.

Gelb, A. (1974). *Applied Optimal Estimation*. A. Gelb.

Ghanes, M., Leon, J.D., and Glumineau, A. (2006). Observability study and observer-based interconnected form for sensorless induction motor. In *Decision and Control, 2006 45th IEEE Conference on*, 1240–1245.

Hermann, R. and Krener, A. (1977). Nonlinear controllability and observability. *IEEE Transactions on Automatic Control*, 22(5), 728–740.

Kalman, R. (1960). A new approach to linear filtering and prediction problems. *Transactions of the ASME - Journal of Basic Engineering*, 82, 35–45.

Kim, S. and Sul, S.K. (2011). Sensorless control of ac motor - where are we now? In *Electrical Machines and Systems (ICEMS), 2011 International Conference on*, 1–6. doi:10.1109/ICEMS.2011.6073316.

Krener, A.J. and Ide, K. (2009). Measures of unobservability. In *Decision and Control, Proceedings of the 48th IEEE Conference on*, 6401–6406.

Lall, S., Marsden, J.E., and Glavaski, S. (2002). A subspace approach to balanced truncation for model reduction of nonlinear control systems. *International Journal on Robust and Nonlinear Control*, 12, 519–535.

Lefebvre, G., Le Digarcher, V., Gauthier, J.Y., Hijazi, A., and Lin-Shi, X. (2015). Optimal low-stator-frequency avoidance strategy to improve the performances of induction machines sensorless drives. In *Sensorless Control for Electrical Drives (SLED), 2015 IEEE Symposium on*, 1–6. doi:10.1109/SLED.2015.7339256.

Lefebvre, G., Gauthier, J.Y., Hijazi, A., Lin-Shi, X., and Le Digarcher, V. (2016). Observability-Index Based Control Strategy for Induction Machine Sensorless Drive at Low Speed. *IEEE Transactions on Industrial Electronics*, 2016. doi:10.1109/TIE.2016.2619662.

Leonhard, W. (1990). Control of Electrical Drivers. *Springer-Verlag*.

Luenberger, D. (1963). Observing the state of a linear system. *IEEE Transactions on Military Electronics*, April, 74–80.

Müller, P. and Weber, H. (1972). Analysis and optimization of certain qualities of controllability and observability for linear dynamical systems. *Automatica*, 8(3), 237–246. doi:10.1016/0005-1098(72)90044-1.

Qian, J., Nadri, M., Morosan, P.D., and Dufour, P. (2014). Closed loop optimal experiment design for on-line parameter estimation. In *Control Conference (ECC), 2014 European*, 1813–1818. doi:10.1109/ECC.2014.6862468.

Singh, A.K. and Hahn, J. (2006). Sensor location for stable nonlinear dynamic systems : Multiple sensors case. *Industrial & Engineering Chemistry Research*, 45, 3615–3623. doi:10.1021/ie0511175.

Sussmann, H.J. (1976). Existence and uniqueness of minimal realizations of nonlinear systems. *Mathematical Systems Theory*, 10(1), 263-284.

Tamai, S., Sugimoto, H., and Yano, M. (1985). Speed sensor-less vector control of induction motor applied model reference adaptive system. In *Conference Record IEEE/IAS Annual Meeting*.

Vaclavek, P., Blaha, P., and Herman, I. (2013). Ac drive observability analysis. *IEEE Transactions on Industrial Electronics*, 60(8), 3047–3059. doi:10.1109/TIE.2012.2203775.